Acta Crystallographica Section F
Structural Biology and Crystallization Communications
ISSN 1744-3091

Crystallization and preliminary X-ray data analysis of β-alanine synthase from *Drosophila melanogaster*

Stina Lundgren,[a] Birgit Andersen,[b] Jure Piškur[b] and Doreen Dobritzsch[a]*

[a]Department of Medical Biochemistry and Biophysics, Karolinska Institute, Stockholm, Sweden, and [b]Department of Organism and Cell Biology, Lund University, Lund, Sweden

Correspondence e-mail: doreen.dobritzsch@ki.se

Received 30 July 2007
Accepted 3 September 2007

β-Alanine synthase catalyzes the last step in the reductive degradation pathway for uracil and thymine, which represents the main clearance route for the widely used anticancer drug 5-fluorouracil. Crystals of the recombinant enzyme from *Drosophila melanogaster*, which is closely related to the human enzyme, were obtained by the hanging-drop vapour-diffusion method. They diffracted to 3.3 Å at a synchrotron-radiation source, belong to space group *C*2 (unit-cell parameters a = 278.9, b = 95.0, c = 199.3 Å, β = 125.8°) and contain 8–10 molecules per asymmetric unit.

1. Introduction

β-Alanine synthase (βAS; EC 3.5.1.6), also called β-ureidopropionase or *N*-carbamyl-β-alanine amidohydrolase, catalyzes the last of the three reactions of the reductive degradation pathway for uracil and thymine: the hydrolysis of *N*-carbamyl-β-alanine and *N*-carbamyl-β-amino isobutyrate to the corresponding β-amino acids (Wasternack, 1980; Piškur *et al.*, 2007). The first two steps are catalyzed by dihydropyrimidine dehydrogenase (EC 1.3.1.2) and dihydropyrimidinase (EC 3.5.2.2), respectively.

The pathway participates in the regulation of the cellular pyrimidine pool, which supplies precursors for nucleotide and nucleic acid synthesis. It is also the main clearance route for the cytotoxic pyrimidine analogue 5-fluorouracil, which is widely used for the treatment of common tumours such as colorectal, head/neck and breast cancer (Heggie *et al.*, 1987). The enzymes of the reductive pyrimidine catabolic pathway rapidly degrade more than 80% of the administered 5-fluorouracil dose and have a considerable influence on the efficacy and pharmacokinetics of this antitumour agent (Milano & Etienne, 1994). Furthermore, the degradation of uracil is the main endogenous source of β-alanine in mammals (Traut & Jones, 1996). This β-amino acid is structurally analogous to the inhibitory neurotransmitters glycine and γ-aminobutyric acid (GABA) and several lines of evidence indicate that it modulates neuronal activity in various parts of the central nervous system (Wang *et al.*, 2003; Sandberg & Jacobson, 1981; Toggenburger *et al.*, 1982). β-Alanine is also a building block of carnosine and anserine, dipeptidic antiglycation agents that have a putative role in protecting the central nervous system against diverse types of pathology such as β-amyloid aggregation (Münch *et al.*, 1997; Hipkiss *et al.*, 1997). The first case of β-alanine synthase deficiency, caused by deletions in the corresponding gene (*UPB1*), was described by Moolenaar *et al.* (2001). The 11-month-old girl concerned showed severe developmental delay and dystonic movement disorders. Additional cases have been reported since which, similar to deficiencies in the other two pyrimidine-degrading enzymes, are associated with neurological disorders and seizures (van Kuilenburg *et al.*, 2004; van Gennip *et al.*, 1997). Bacteria, yeast and plants use β-alanine for the biosynthesis of pantothenic acid (vitamin B_5; Cronan *et al.*, 1982).

Eukaryotic βAS has been purified and characterized from a number of sources (Sanno *et al.*, 1970; Wasternack *et al.*, 1979; Tamaki *et al.*, 1987; Gojković *et al.*, 2001; Walsh *et al.*, 2001; Waldmann *et al.*, 2005). Their subunit molecular weights range from 42 to 50 kDa. Phylogenetic analyses revealed that they can be assigned to two

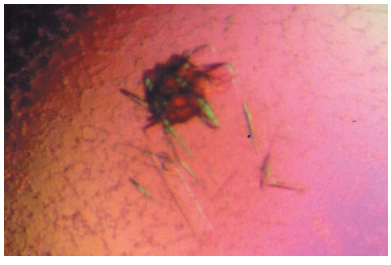

subfamilies (Gojković *et al.*, 2001), with the majority of the eukaryotic enzymes, including those from human, calf, rat and fruit fly, forming one of them. The enzyme from the yeast *Saccharomyces kluyveri*, to date the only βAS with known crystal structure (Dobritzsch *et al.*, 2003; Lundgren *et al.*, 2003), shows no sequence similarity to this group but is related to bacterial *N*-carbamyl-L-amino-acid amidohydrolases, hence forming a separate subfamily. It is a dimer of identical subunits comprising two domains with α/β topology, the larger of which contains a di-zinc centre that is essential for catalytic activity.

Owing to the dissimilarity of the amino-acid sequences, we expect the fold of βAS from *Drosophila melanogaster* to be unrelated to that of yeast βAS. In contrast, its 64% identity to the amino-acid sequence of human βAS suggests a close structural relationship and the crystal structure of the fruit-fly enzyme could therefore serve as a model for the human counterpart. Of proteins of known crystal structure, the primary sequence of the homotetrameric *N*-carbamyl-D-amino-acid amidohydrolase shows the highest homology to fruit-fly βAS (24% identity, 43% homology). Its subunit structure comprises a sandwich of parallel β-sheets surrounded by two layers of α-helices (Nakai *et al.*, 2000). Like βAS, *N*-carbamyl-D-amino-acid amidohydrolase catalyzes the hydrolytic cleavage of an *N*-carbamyl group from its substrate. It does not contain any metal ions, but utilizes a nucleophilic chemical mechanism in which a cysteine thiol acts as the nucleophile and a glutamate/lysine pair as acid-base catalysts. This triad of catalytic residues is conserved in the higher eukaryotic βAS, suggesting that the reaction proceeds according to a similar mechanism and does not involve the activation of a water molecule by a di-zinc centre as seen in yeast βAS. Although rat liver and maize βAS have been shown to contain zinc ions (Kvalnes-Krick & Traut, 1993; Walsh *et al.*, 2001), the zinc-ligating residues of the yeast enzyme are not conserved. Hence, potential metal binding is most likely to be achieved in a different way and to have a different function.

Allosteric behaviour has been observed for rat liver βAS, which changes oligomeric state in response to effector molecules from a stable active homohexamer to either an inactive homotrimer (in the presence of the product β-alanine) or an active homododecamer (in the presence of the substrate *N*-carbamyl-β-alanine) (Matthews & Traut, 1987). The enzymes from *Arabidopsis thaliana* and *Zea mays* form homodecamers (Walsh *et al.*, 2001), while the native state of calf liver βAS is a homohexamer (Waldmann *et al.*, 2005).

Here, we report the crystallization and preliminary X-ray diffraction data analysis of the first member of the subfamily of βASs from higher eukaryotes, *i.e.* the enzyme from *D. melanogaster*.

2. Experimental procedures

2.1. Protein expression and purification

βAS from *D. melanogaster* was recombinantly expressed with a C-terminal His_8 tag (FPGDDDDKHHHHHHHHSGD), which extended the polypeptide chain by 19 residues to 405 amino acids. The calculated molecular weight of the tagged monomer is 46.1 kDa and the theoretical isoelectric point is 6.24. Expression and purification using an Ni^{2+}–NTA column (Qiagen) was performed as described previously (Gojković *et al.*, 2001), but with some modifications to increase the homogeneity of the purified protein. DNA was removed prior to the affinity-chromatography step *via* streptomycin precipitation [2%(*w*/*v*) final concentration in the lysate]. Furthermore, the pooled protein-containing fractions eluted from the Ni^{2+}–NTA column were precipitated with ammonium sulfate (70% saturation at 277 K, centrifugation at 24 500*g* for 30 min at 277 K) and the redissolved pellet was applied onto an S-12 gel-filtration column (20 ml, GE Healthcare) equilibrated with 100 m*M* sodium phosphate pH 7.0, 10%(*w*/*v*) glycerol. Elution of the protein was achieved at a flow rate of 0.5 ml min^{-1} with the same buffer. Fractions containing fruit-fly βAS were pooled and the buffer was exchanged to 50 m*M* HEPES pH 7.5, 100 m*M* NaCl, 1 m*M* DTT (storage buffer) by repeated steps of centrifugation at 6000*g* in a Microsep Centrifugal Concentrator (Pall Corporation) and subsequent dilution of the sample with storage buffer. After the last dilution, the protein was concentrated to a final concentration of 15–20 mg ml^{-1}. *D. melanogaster* βAS was aliquoted and stored at 193 K until further use.

2.2. Crystallization

The crystallization of *D. melanogaster* βAS was attempted using several commercially available sparse-matrix and grid screens (Hampton Research, Molecular Dimensions, Emerald BioSystems). Crystallizations were set up at 293 K using the vapour-diffusion method with sitting drops in 96-well plates. The drops contained 1 µl each of protein and reservoir solution; the protein concentration was varied between 4 and 10 mg ml^{-1}. No crystalline material was obtained in the first round of setups. The experiments were repeated with protein solutions containing various additives, *e.g.* 0.2%(*w*/*v*) β-octylglucoside, 5 m*M* *N*-carbamyl-β-alanine (substrate) and 5%(*v*/*v*) glycerol or 5 m*M* β-alanine (product) and 5%(*v*/*v*) glycerol. After one month of equilibration at 293 K, small crystals appeared under two conditions from the Wizard I and II screens (Emerald BioSystems), 30%(*w*/*v*) PEG 400, 0.1 *M* CHES pH 9.5 and 10%(*w*/*v*) PEG 3000, 0.1 *M* phosphate–citrate pH 4.2, 0.2 *M* NaCl, when 5 m*M* *N*-carbamyl-β-alanine and 5%(*v*/*v*) glycerol were present in the protein solution. Both conditions are very different from those that resulted in the crystallization of *S. kluyveri* βAS (Dobritzsch *et al.*, 2003). The latter condition was optimized using 24-well hanging-drop plates. The best crystals were obtained using vapour diffusion against a reservoir containing 1 ml 9–12%(*w*/*v*) PEG 3350, 0.1 *M* phosphate–citrate pH 4.2 and 0.2 *M* NaCl. The 4 µl droplets consisted of equal volumes of protein solution [6–12 mg ml^{-1} βAS, 5 m*M* *N*-carbamyl-β-alanine and 5%(*v*/*v*) glycerol in storage buffer] and mother liquor. Crystals of fruit-fly βAS (Fig. 1) appeared after 14–30 d equilibration at 293 K after the drops had undergone some kind of metamorphosis: they remained clear for a few days, after which a glistening micro-

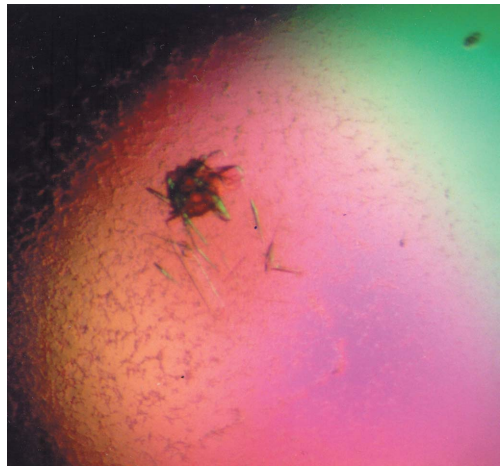

Figure 1
Crystals of *D. melanogaster* βAS grown by the hanging-drop method.

crystalline precipitate formed which acquired a mesh-like structure after another 2–3 d. Clusters of crystals formed from this structured precipitate in about half of the drops, but less than 10% of them appeared to be ordered enough to be utilized in diffraction experiments. The crystals reached maximum dimensions of 0.15 × 0.05 × 0.02 mm and about 1–2 months after appearance they started to show clear signs of aging such as rounding of the edges. SDS–PAGE was performed with samples of *D. melanogaster* βAS before and after crystallization. It revealed identical molecular sizes for both samples and therefore excluded the occurrence of proteolytic cleavage of the enzyme after set-up of the drops (Fig. 2), which may have accounted for the peculiar crystallization behaviour.

Attempts to improve the success rate of crystallization and the quality of the crystals using these conditions did not give the desired result, but no attempt has yet been made to improve the crystallization outcome by removal of the His_8 tag. Furthermore, crystals obtained using the other conditions identified in the initial screens could not be reproduced, nor could other crystallization conditions be found. It is also noteworthy that no crystals were obtained from the optimized condition in the absence of substrate. The addition of glycerol was also essential and a higher crystallization success rate was observed when it was added to the protein solution instead of the reservoir solution.

2.3. Data collection and processing

Before data collection, crystals were transferred for about 5 s into a 2 µl drop of cryosolution, which consisted of mother liquor supplemented with 25%(*w*/*v*) PEG 400. The crystals were flash-frozen in a cold nitrogen stream at 100 K. X-ray diffraction data were collected at beamline ID23-1 at the ESRF (Grenoble, France) using an ADSC Quantum Q315R detector. Crystals of fruit-fly βAS diffracted poorly and in nine out of ten cases with high anisotropy and high mosaic spread (>1°), rendering most of them unsuitable for data collection. Data corresponding to a total of 225° were eventually collected from a crystal that diffracted to a maximum of 2.8 Å at a wavelength of 0.939 Å, using a crystal-to-detector distance of 477 mm and an oscillation angle of 0.5°. Integration of the diffraction data was carried out with *MOSFLM* (Leslie, 1992). Intensities were merged and scaled using *SCALA* and structure factors were calculated with *TRUNCATE* from the *CCP*4 suite of programs (Collaborative Computational Project, Number 4, 1994).

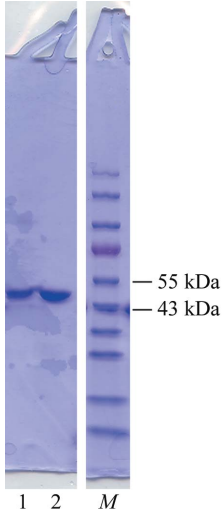

Figure 2
SDS–PAGE of *D. melanogaster* βAS samples. Lane 1, crystals collected from one hanging drop redissolved in water; lane 2, before crystallization; lane *M*, prestained protein ladder (Fermentas).

Table 1
Diffraction, data-collection and reduction statistics.

Values in parentheses are for the highest resolution shell.

Wavelength (Å)	0.939
Space group	*C*2
Unit-cell parameters (Å, °)	*a* = 278.9, *b* = 95.0, *c* = 199.3, β = 125.8
Resolution limits (Å)	50.0–3.3 (3.48–3.30)
No. of reflections	133885 (17765)
No. of unique reflections	54793 (7508)
R_{sym} (%)	17.1 (38.5)
Mean $I/\sigma(I)$	6.4 (2.1)
Completeness (%)	86.0 (81.2)
Multiplicity	2.4 (2.4)

3. Results and discussion

Autoindexing indicated that the crystals of *D. melanogaster* βAS belonged to the monoclinic space group *C*2, with unit-cell parameters *a* = 278.9, *b* = 95.0, *c* = 199.3 Å, β = 125.8°. The asymmetric unit is likely to contain 8–10 polypeptide chains, which corresponds to a solvent content of 57.6–47.0% and a Matthews coefficient of 2.9–2.3 $Å^3\ Da^{-1}$ (Matthews, 1968). The native quaternary structure of fruit-fly βAS is as yet undetermined. Native gel electrophoresis experiments show a mixture of oligomeric states (the smallest of which is most likely to represent a dimer), while analysis by analytical gel filtration suggests an oligomer composed of eight or more polypeptide chains (data not shown). Hence, the asymmetric unit of the crystals may contain one, two or four biological units of *D. melanogaster* βAS.

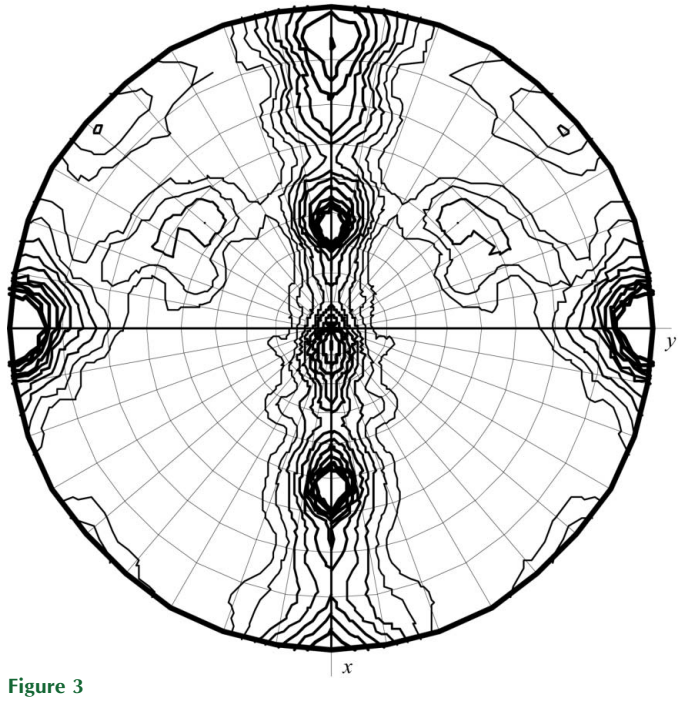

Figure 3
Self-rotation function (χ = 180°) calculated using the program *MOLREP* (Vagin & Teplyakov, 1997) based on crystallographic data from 49.0 to 3.4 Å resolution obtained for *D. melanogaster* βAS. The labelling of the *x* and *y* axes is according to the orthogonal coordinate system defined by *MOLREP*.

During data processing, it became evident that the anisotropic diffraction and rapid decay of the crystal in the X-ray beam made it necessary to discard all data with resolution beyond 3.3 Å and that only 165° of the data could be used. The significant anisotropy contributes to the high $R_{\rm sym}$ of 17.7% observed for the whole data set and the low completeness of the higher resolution shells. Further data statistics are given in Table 1.

Calculation of the native Patterson map revealed a peak in the $v = 0$ section at position (0, 0, 0.186) with about 15% of the height of the origin peak; however, this may not be significant enough to indicate pseudo-translational symmetry. A self-rotation function was calculated with the program *MOLREP* (Vagin & Teplyakov, 1997). The $\chi = 180°$ section of the map, calculated with an integration radius of 30 Å using data in the resolution range 49.0–3.4 Å, shows one peak with 78.5% of the height of the origin peak ($\theta = 126.0$, $\varphi = 180.0°$) and several additional peaks with 26–46% of the height of the origin peak, indicating the presence of a number of noncrystallographic twofold axes (Fig. 3).

Determination of the crystal structure of *D. melanogaster* βAS was attempted by molecular replacement using the programs *MOLREP* (Vagin & Teplyakov, 1997), *Phaser* (McCoy *et al.*, 2007), *EPMR* (Kissinger *et al.*, 1999) and *AMoRe* (Navaza, 1994). As expected, utilization of a subunit of yeast βAS (PDB code 1r3n) as the search model remained unsuccessful. In subsequent trials, the crystal structures of *N*-carbamyl-D-amino-acid amidohydrolase (PDB code 1erz; 24% amino-acid sequence identity; Nakai *et al.*, 2000) and of the hypothetical protein PH0642 from *Pyrococcus horikoshii* (PDB code 1j31; 28% identity; Sakai *et al.*, 2004) served as search models in the monomeric, dimeric or tetrameric state and at diverse levels of sequence adjustment and truncation. However, no clear molecular-replacement solution has yet been obtained. The expression of selenomethionine-substituted fruit-fly βAS is under way in order to allow the determination of its crystal structure by MAD phasing techniques. Meanwhile, efforts to obtain phases by molecular replacement are continuing.

We thankfully acknowledge access to the synchrotron-radiation facilities and support from the staff at the European Synchrotron Radiation Facility (Grenoble, France), at the Deutsches Elektronen Synchrotron (Hamburg, Germany) and at MAX-lab (Lund, Sweden). This work was supported by grants from the Swedish Research Council, the Swedish Cancerfonden, Åke Wibergs Stiftelse, Karolinska Institute Foundation and Stiftelse Lars Hiertas Minne.

References

Collaborative Computational Project, Number 4 (1994). *Acta Cryst.* D**50**, 760–763.
Cronan, J. E., Littel, K. J. & Jackowski, S. (1982). *J. Bacteriol.* **149**, 916–922.
Dobritzsch, D., Gojković, Z., Andersen, B. & Piškur, J. (2003). *Acta Cryst.* D**59**, 1267–1269.
Gennip, A. H. van, Abeling, N. G., Vreken, P. & van Kuilenburg, A. B. (1997). *J. Inherit. Metab. Dis.* **20**, 203–213.
Gojković, Z., Sandrini, M. P. B. & Piškur, J. (2001). *Genetics*, **158**, 999–1011.
Heggie, G. D., Sommadossi, J. P., Cross, D. S., Huster, W. J. & Diasio, R. B. (1987). *Cancer Res.* **47**, 2203–2206.
Hipkiss, A. R., Preston, J. E., Himswoth, D. T., Worthington, V. C. & Abbot, N. J. (1997). *Neurosci. Lett.* **238**, 135–138.
Kissinger, C. R., Gehlhaar, D. K. & Fogel, D. B. (1999). *Acta Cryst.* D**55**, 484–491.
Kuilenburg, A.B. van *et al.* (2004). *Hum. Mol. Genet.* **13**, 2793–2801.
Kvalnes-Krick, K. L. & Traut, T. W. (1993). *J. Biol. Chem.* **268**, 5686–5693.
Leslie, A. G. W. (1992). *Jnt CCP4/ESF–EACBM Newsl. Protein Crystallogr.* **26**.
Lundgren, S., Gojković, Z., Piškur, J. & Dobritzsch, D. (2003). *J. Biol. Chem.* **51**, 51851–51862.
McCoy, A. J., Grosse-Kunstleve, R. W., Adams, P. D., Winn, M. D., Storoni, L. C. & Read, R. J. (2007). *J. Appl. Cryst.* **40**, 658–674.
Matthews, B. W. (1968). *J. Mol. Biol.* **33**, 491–497.
Matthews, M. M. & Traut, T. W. (1987). *J. Biol. Chem.* **262**, 7232–7237.
Milano, G. & Etienne, M.-C. (1994). *Pharmacogenetics*, **4**, 301–306.
Moolenaar, S. H., Gohlich-Ratmann, G., Engelke, U. F. H., Spraul, M., Humpfer, E., Dvortsak, P., Voit, T., Hoffmann, G. F., Brautigam, C., van Kuilenburg, A. B. P., van Gennip, A. H., Vreken, P. & Wevers, R. A. (2001). *Magn. Reson. Med.* **46**, 1014–1017.
Münch, G., Mayer, S., Michaelis, J., Hipkiss, A. R., Riederer, P., Muller, R., Neumann, A., Schinzel, R. & Cunningham, A. M. (1997). *Biochim. Biophys. Acta*, **1360**, 17–29.
Nakai, T., Hasegawa, T., Yamashita, E., Yamamoto, M., Kumasaka, T., Ueki, T., Nanba, H., Ikenaka, Y., Takahashi, S., Sato, M. & Tsukihara, T. (2000). *Structure*, **8**, 729–739.
Navaza, J. (1994). *Acta Cryst.* A**50**, 157–163.
Piškur, J., Schnackerz, K. D., Andersen, G. & Björnberg, O. (2007). *Trends Genet.* **23**, 369–372.
Sakai, N., Tajika, Y., Yao, M., Watanabe, N. & Tanaka, I. (2004). *Proteins*, **57**, 869–873.
Sandberg, M. & Jacobson, I. (1981). *J. Neurochem.* **37**, 1353–1356.
Sanno, Y., Holzer, M. & Schimke, R. T. (1970). *J. Biol. Chem.* **245**, 5668–5676.
Tamaki, N., Mizutani, N., Kikugawa, M., Fujimoto, S. & Mizota, C. (1987). *Eur. J. Biochem.* **169**, 21–26.
Toggenburger, G., Felix, D., Cuenod, M. & Henke, H. (1982). *J. Neurochem.* **39**, 176–183.
Traut, T. W. & Jones, M. E. (1996). *Prog. Nucleic Acid Res. Mol. Biol.* **53**, 1–78.
Vagin, A. & Teplyakov, A. (1997). *J. Appl. Cryst.* **30**, 1022–1025.
Waldmann, G., Cook, P. F. & Schnackerz, K. D. (2005). *Protein Pept. Lett.* **12**, 69–73.
Walsh, T. A., Green, S. B., Larrinua, I. M. & Schmitzer, P. R. (2001). *Plant Physiol.* **125**, 1001–1011.
Wang, D. S., Zhu, H. L. & Li, J. S. (2003). *Int. J. Neurosci.* **113**, 293–305.
Wasternack, C. (1980). *Pharmacol. Ther.* **8**, 629–651.
Wasternack, C., Lippmann, G. & Reinbotte, H. (1979). *Biochim. Biophys. Acta*, **570**, 341–351.